Laser-triggered hollow-cathode plasma process for film growth

S. Witanachchi,[a] P. Mahawela, and P. Mukherjee
Department of Physics, Laboratory for Advanced Materials Science and Technology (LAMSAT), University of South Florida, Tampa, Florida 33620

(Received 12 February 2004; accepted 28 June 2004; published 23 September 2004)

A method of generating a pulsed plasma plume of metallic species using a hollow-cathode arc discharge arrangement is presented. Electrical energy from a pulse-forming network (PFN) generates the transient plasma that evaporates material from the anode that is placed inside a hollow cathode. The discharge is triggered by thermionic electrons produced by a CO_2 laser pulse that impinges on one of the electrodes. This plasma process has been used to deposit carbon films in a low-pressure argon or nitrogen ambient. Current pulses of 4–10 ms in duration with peak currents of 350 A have been produced by the PFN. Characteristics of the produced plasma have been studied by optical emission spectroscopy. The amount of energy imparted to the argon plasma is more than that for a nitrogen plasma. Comparison of on-axis intensity for the 426.9 nm line of C^+ for the two plasmas shows that the density of carbon ions generated in the nitrogen plasma is higher than that in the argon plasma. Films deposited by this method have fairly uniform thickness profiles that are of the form $\cos^{0.4}\theta$ for the argon plasma and $\cos^{2.2}\theta$ for the nitrogen plasma. This indicates that the nitrogen plasma is more forward directed than the argon plasma. Deposition rates of about 10–16 Å/pulse have been obtained for carbon films. © *2004 American Vacuum Society.* [DOI: 10.1116/1.1784828]

I. INTRODUCTION

The advantages offered by the collisions of energetic species during film growth are well understood. Depositing species in the energy range of 3–50 eV has been known to alter the crystallographic and physical properties such as substrate–film adhesion, density, surface roughness, film stress, and growth orientation.[1–4] In addition, high flux of energetic collisions at the substrate can potentially increase the density of nucleation sites on the substrate leading to smaller, even nanosize grain growth. Hardness of films, as described by the Hall–Petch relation,[5] is expected to be enhanced by the presence of nanograins. Therefore, a source that is capable of producing a high flux of energetic species will play an important role in the fabrication of hard coatings. Also, ionic plumes can be easily manipulated by external electric and magnetic fields. For this reason, deposition of material from ionic plasma plumes offers the advantageous capability of guidance into narrow microtrenches or vias. Most neutrals, on the other hand, enter trenches and vias at large angles leading to sidewall growth of the structures.[6]

Energetic species have been exploited in several film growth processes. These techniques include ion beam assisted deposition (IBAD),[7] filtered vacuum arc deposition,[8,9] and laser ablation.[10,11] In the IBAD process, the neutral atoms of the depositing species are generated by an evaporation process while the substrate is simultaneously bombarded with a directed gaseous ion source. Vacuum arcs are mostly operated under microdischarge conditions and thus produce microparticles. Elaborate magnetic field guiding systems are typically incorporated to filter out the undesirable particulates. Plumes produced by single laser ablation contain highly excited neutrals, while the percentage of ionization can be as low as 8%.[12] On the other hand, the percentage of ionization in dual-laser ablated plumes can be over 70%.[13] While dual-laser ablation enhances plume ionization and simultaneously affects the possibility of large-area, uniform film deposition, it causes a reduction in the deposition rate compared to conventional single laser ablation. In this article we report on a hollow-cathode plasma system that has the capability to produce highly ionized plumes of metallic species that enable the growth of uniform large-area films at high growth rates. We have used this technique with carbon electrodes to study the growth of carbon films.

II. EXPERIMENT

Arc plasma sources can be operated in either continuous or pulsed mode. Pulsed plasma sources have the advantage of generating low thermal loads and peak currents as high as 1 kA. High current, which increases the power density, also leads to plasmas that are more than 90% ionized.[14,15] In typical pulsed plasmas the arc is ignited and extinguished using a high-voltage electronic trigger pulse.[16] However, in high voltage operation of the arc the material is removed from the electrodes by microdischarges that produce high density of particulates.[17] In this article we report on a pulsed CO_2 laser triggering technique that enables the operation of distributed pulsed plasma at a low discharge voltage. Unlike the plasmas operated in the microdischarge mode, the distributed discharges suppress particulate ejection.[18]

The hollow-cathode system consists of a cylindrical carbon tube about 1 cm in diameter and 2 cm in length as the cathode, and a 3–5 mm diam long solid carbon rod as the

[a]Author to whom correspondence should be addressed; electronic mail: switanac@cas.usf.edu

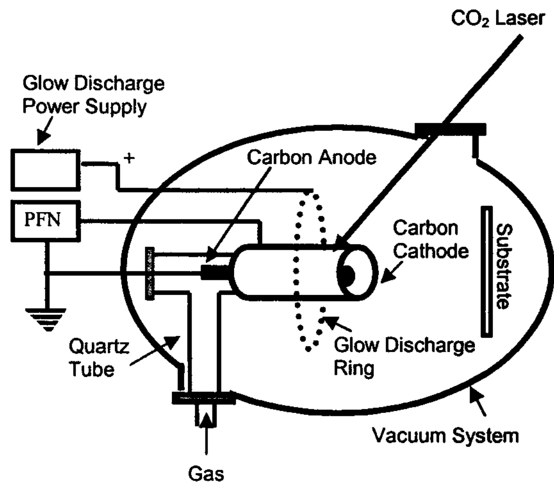

FIG. 1. Schematic diagram of the laser-triggered hollow-cathode plasma deposition system.

anode. The carbon tube and the rod are placed concentrically through a quartz tube that allowed gas flow through the hollow cathode. A pulse-forming network (PFN) that consists of capacitive and inductive elements is connected across the anode and the grounded cathode. The PFN is operated at a low voltage of 50–70 V and can impart 1–20 J of energy into the plasma. A schematic of the hollow-cathode system is shown in Fig. 1. Triggering of the discharge at this low voltage requires preionization of the ambient gas near the electrodes. A ring electrode of about 6 cm in diameter that is positively biased (at 200–600 V) is placed around the cathode tube to generate an auxiliary glow discharge of an inert gas or a reactive gas (such as nitrogen). The thermionic electrons that are generated when a CO_2 laser pulse of 40–80 mJ energy and 200 ns pulse duration is incident on the outer surface of the carbon cathode tube initiate the glow discharge and trigger the PFN in turn. The glow discharge voltage is synchronized such that the glow is pulsed between laser pulses. The high impedance power supply used for the glow discharge maintained the peak current below 10 mA. Discharge of the PFN generates a highly ionized plasma that causes the cathode tube to erode through ion bombardment. The anode is also heated by electron bombardment. However, the temperature rise is not sufficient to evaporate carbon from the carbon anode. Evaporated atoms within the hollow cathode are further ionized by electron impact ionization during the current pulse. Due to the high pressure of the plasma generated within the cathode tube the plasma plume expands rapidly out of the hollow cathode.

In this study we have investigated the plasma characteristics and carbon film growth in argon and nitrogen as ambient gases. The amount of energy imparted to the plasma from the PFN is primarily dependant on the storage capacitor and the change in the output voltage during the discharge. In addition, the energy delivered to the hollow-cathode plasma also depended on the type of gas as well as the gas pressure. In our experiments, the discharge characteristics of the plasma are determined by measuring the current pulses produced by the PFN. A calibrated inductively coupled pick-up coil is used to record the current pulse on a fast oscilloscope. The PFN is charged up to a voltage of 70 V and the plasma is triggered at the rate of 1 Hz using the pulsed CO_2 laser. The voltage of the capacitor before and after the discharge is used to compute the total energy imparted to the plasma in a current pulse. In this computation it is assumed that all the energy discharged from the capacitor is directed to the plasma. However, in practice some percentage of the energy may dissipate through other mechanisms. These experiments were carried out for different pressures of argon and nitrogen, and for different values of storage capacitances to determine their effect on the plasma characteristics.

When the electrical energy coupled into the plasma increases, the added energy can either be channeled into the gas resulting in the increased ionization of only the gas atoms, or the energy can increase the evaporation of carbon that would lead to increased growth rate. To determine the density of carbon ions present in the plasma under different conditions a species-resolved detection technique is required. In our experiments the ionic content of the generated plasma was investigated by emission spectroscopy. An estimation of ion densities from the emission lines requires careful calibration of the peaks in conjunction with ion mass analysis. However, line intensities of two spectra corresponding to specific ionic states can be compared to qualitatively gauge the change in the plasma ionic content. An optical multichannel analyzer (OMA) equipped with a fiber optic cable for light input was used to obtain the emission spectrum of the plasma. The plasma plume was imaged onto a focal plane where the optical fiber was placed to collect emission from a point on the axis of the plume at a distance of 4 cm from the electrodes. Emission lines corresponding to singly and multiply ionized carbon were monitored for different pressures and different values of the storage capacitors for argon and nitrogen.

The expansion of the plasma subsequent to the discharge is mainly pressure driven. The high density of the plasma inside the cathode tube gives rise to a relatively higher pressure inside compared to that outside. Due to significantly high gas collisions, the expansion profile is not expected to be highly forward directed. Formation of the carbon plasma was observed by imaging the plume emission on to a time-gated charge coupled device (CCD) camera. The initial development of the plasma was recorded with time delays in the millisecond time scale with a 1 μs gate width. Imaging the plasma with a 3 nm band pass interference filter centered at 426 nm enabled us to observe the dynamics of the carbon ion emission at 426.73 nm without interference due to the emission from argon. The closest high intensity argon line (at 434.8 nm) is outside the range of the band pass filter. To determine the thickness profiles of the carbon films produced by this process, films were deposited on 3 in. silicon wafers placed 5 cm from the plasma source. Amorphous carbon films were deposited at room temperature in both argon and nitrogen at a 3 mT pressure with the same PFN capacitor of 34 mF at 70 V.

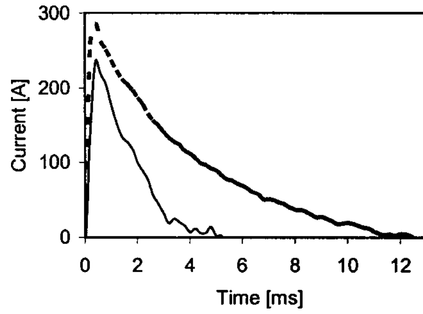

FIG. 2. Inductively measured current pulses produced by the PFN discharge for argon and nitrogen carrier gases at 2 mTorr background pressure.

III. RESULTS AND DISCUSSION

A. Discharge characteristics

Operation of the electrodes at low voltage facilitated the formation of a distributed discharge within the hollow cathode. The distributed discharge condition helps to reduce particulate ejection that is common in microdischarges.[18] When microdischarges take place, most of the energy in the capacitor is discharged in a few microseconds causing explosive evaporation of the electrodes. The probability of such discharges increases with increasing PFN voltage.[18] Figure 2 shows the transient current pulses produced in 2 mT pressure of argon and nitrogen. Such broad current pulses indicate distributed discharge conditions. The area under the curve represents the total charge drawn from the capacitor during the current pulse. The energy imparted to the plasma is proportional to the square of this charge for a given PFN capacitor. Based on the curves in Fig. 2, the energy transferred to the argon plasma is more than four times that transferred to the nitrogen plasma. The energy transferred to the plasma can also be computed based on the difference between the initial voltage of the PFN storage capacitor and the voltage after the discharge. Figure 3 shows the increase of the energy input to the plasma with increasing gas pressure. Clearly, more energy is delivered to the argon plasma than the nitrogen plasma. For example, at a pressure of 4 mTorr the transferred energy increased from 10 to 25 J for argon compared to nitrogen. Increasing the PFN capacitance can also increase plasma energy while maintaining the distributed discharge

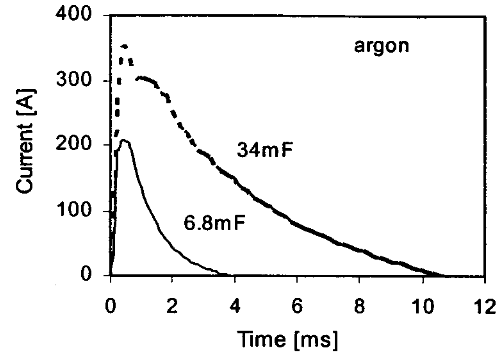

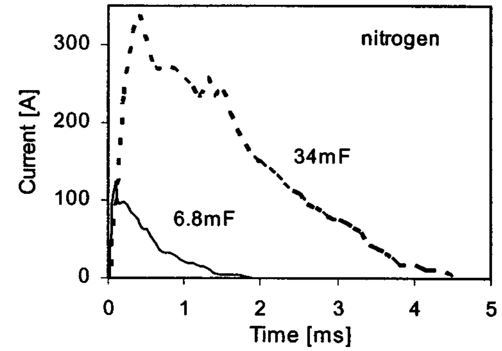

FIG. 4. Inductively measured current pulses for 6.8 and 34 mF capacitors with 2mTorr of argon and nitrogen carrier gases.

conditions. Figure 4 shows the behavior of the current pulse when the capacitance was changed from 6.8 to 34 mF. The broadening of the current pulse with increasing capacitance is expected as a result of the higher discharge time constant. The effect of increasing capacitance on the amount of energy delivered to the plasma is shown in Fig. 5.

B. Multiply ionized carbon in the plasma

The previous experiments show that the energy input to the plasma increases with increasing gas pressure and the capacitance of the PFN. It is desirable for this energy to be channeled for the evaporation of carbon from the electrodes rather than increasing the ionization of the gas. Emission spectroscopy of the plasma helped to gauge the density of carbon in the plasma. Emission spectrum of the plasma was

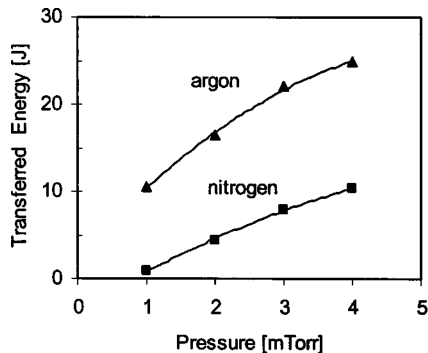

FIG. 3. Total energy transferred to the plasma at different pressures of argon and nitrogen for a 34 mF capacitance.

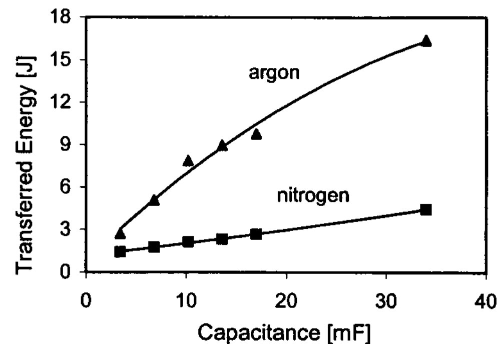

FIG. 5. Total energy transferred to the plasma at different capacitors at 2 mTorr background pressure of argon and nitrogen.

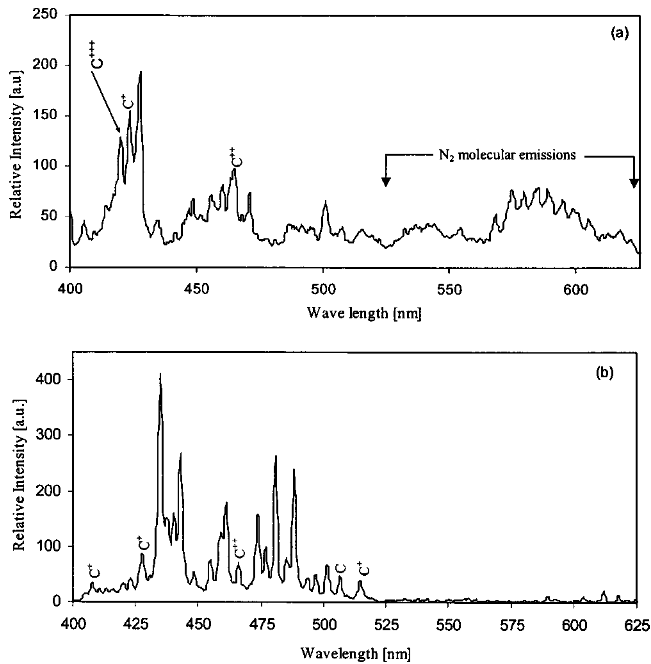

FIG. 6. Emission spectrum recorded by an OMA on-axis at a point 4 cm from the electrode in 2 mTorr of: (a) argon and (b) nitrogen.

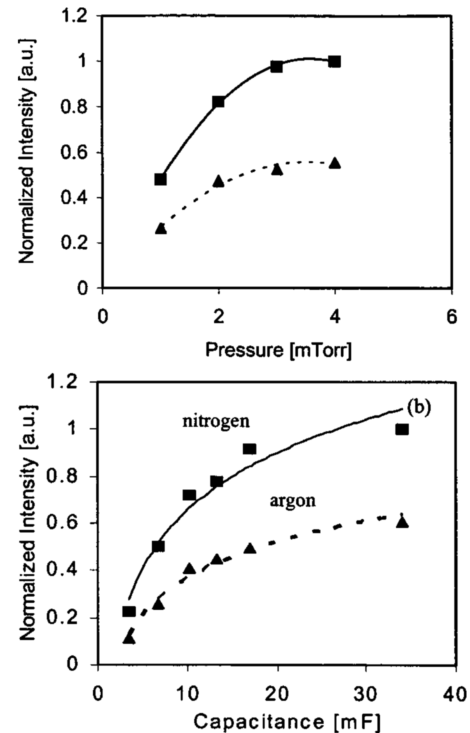

FIG. 7. Emission intensity of the C^+ line at 426.7 nm for argon and nitrogen at: (a) different pressures and (b) different capacitances.

rich in ionic carbon emissions. Change in the signal intensity corresponding to ionic transitions of C^+ at 392.069 and 426.7 nm, C^{2+} at 465.147 nm, and C^{3+} at 419.52 nm were monitored for argon and nitrogen ambient at different pressures. Representative emission spectra of the plasma in nitrogen and argon background are shown in Fig. 6. The emission lines of carbon ions for the argon plasma were dwarfed by the strong emissions from argon. Intensity of the carbon ion lines were observed to increase with increasing gas pressure and increasing capacitance. Pressure and capacitance dependence of the ionic content of the plasma can be seen in Fig. 7. These results demonstrate that the increase in the energy imparted to the plasma mainly goes to evaporate and ionize more carbon from the electrodes while some of the energy is spent in increasing the gas ionization.

C. Film growth profiles

The images of the expanding carbon plasma, recorded by the CCD using the 426 nm filter for transmission of the carbon 426 nm ion line at time delays of 2 and 6 ms with respect to the CO_2 laser are shown in Fig. 8. The plasma was generated with a PFN capacitance of 34 mF with argon as the carrier gas. According to the observed current pulse under these conditions [Fig. 4(a)], 45% of the energy is imparted to the plasma in 2 ms, whereas 95% of the energy is imparted in 6 ms. A significant increase in the carbon ionic content of the plasma within this time period is clear from these CCD images. The measured thickness of the films grown in nitrogen and argon under the same conditions for 300 pulses were 0.58 and 0.36 μm, respectively. This corresponds to an on-axis growth rate in nitrogen of 19 Å/pulse while the rate for argon is 12 Å/pulse. Thickness scans in the x and y direction of the films deposited on silicon substrates in 3 mT pressure of argon and nitrogen are shown in Figs. 9 and 10, respectively. The spatial thickness for the film deposited in argon exhibited a profile of the form $\cos^{0.4}\theta$ in both $x$and y directions, while that for the films deposited in nitrogen was of the form $\cos^{2.2}\theta$. Clearly, the films grown in argon have shown greater uniformity than the films grown in nitrogen. A comparative value of the amount of carbon evaporated in each gas type can be obtained by integrating the area under the two dimensional profile of the films. Based on this computation, the ratio of the total material evaporated in argon (M_{argon}) to nitrogen (M_{nitrogen}) is 1.4.

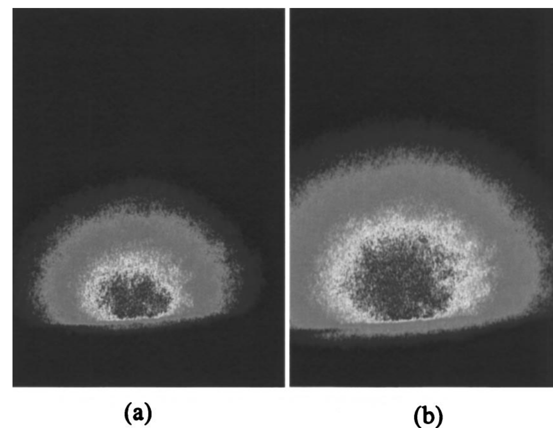

FIG. 8. (Color) CCD images through a 3 nm band pass filter centered at 426.7 nm emission line of C^+ at: (a) 2 ms and (b) 6 ms delays. The CCD was triggered by the onset of the current pulse.

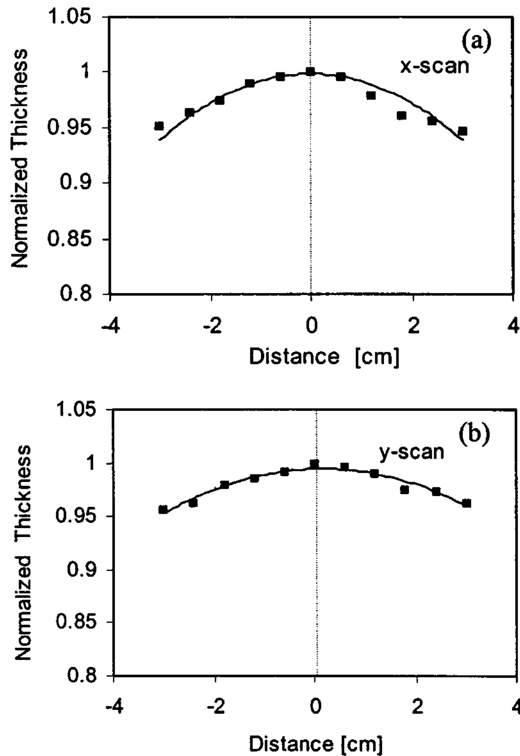

FIG. 9. Normalized thickness profiles of the carbon films deposited on a substrate placed 6 cm from the electrode with argon as the carrier gas: (a) x scan and (b) y scan. On-axis film thickness is 0.36 μm. The fits for both are curves that show a $\cos^{0.4}\theta$ form.

Even though the amount of material evaporated per pulse is higher for the argon plasma, the narrower expansion profile of the nitrogen plasma makes the on-axis density of material higher. This is consistent with the emission spectroscopy results presented in Fig. 7, where on-axis emission is higher for nitrogen than argon.

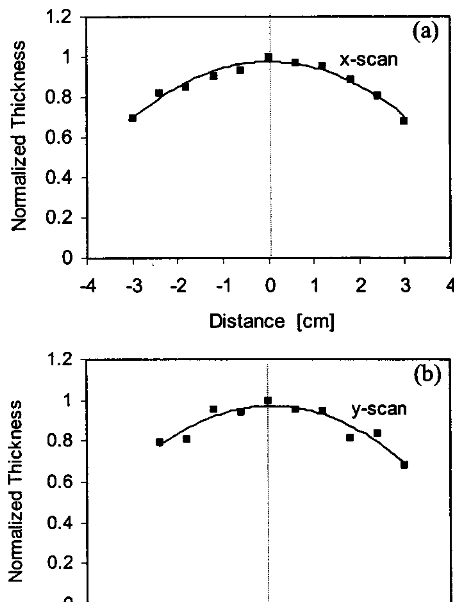

FIG. 10. Normalized thickness profiles of the carbon films deposited on a substrate placed 6 cm from the electrode with nitrogen as the carrier gas: (a) x scan and (b) y scan. On-axis film thickness is 0.58 μm. The fits for both are curves show a $\cos^{2.2}\theta$ form.

IV. CONCLUSION

In this article, we have presented a technique to produce a highly ionized transient plasma plume of metallic species. The hollow-cathode plasma process described in this article offers several advantages for film growth which include high growth rate, relatively small film thickness variation across the substrate, ion-assisted growth leading to enhanced adhesion, and high reactivity. In addition, the transient nature of the growth may be important in processes where modulation of the substrate during or in between the growth cycles is required.

The results demonstrate the use of carbon electrodes to deposit films at a high growth rate in both nitrogen and argon gas ambient. Analysis of the current pulses generated by the PFN shows that more energy is imparted to the argon plasma than the nitrogen plasma under similar deposition and ambient pressure conditions. Optical diagnostics of the plasma detected multiply ionized carbon emissions indicating highly ionized plasma. Comparison of the emission intensity of on-axis carbon ions for the two gases shows that the density of the evaporated species propagating on-axis is higher for nitrogen. However, argon produced much more uniform films than nitrogen, leading to broad film profiles of the form $\cos^{0.4}\theta$. Computation of the total material evaporated with nitrogen and argon shows that, under similar conditions, argon evaporated 1.4 times more material than nitrogen. This result is consistent with more energy being imparted to the plasma when argon is the carrier gas, as shown in Fig. 3. Furthermore, the expansion profiles produced by the nitrogen plasma are more forward-directed, and therefore the density of material on-axis is higher than that for the argon plasma. This result is also consistent with the emission spectroscopy results where the on-axis emission intensity of the carbon ions for nitrogen is higher than that for argon (Fig. 7). If the efficiency of the hollow cathode plasma process is to be compared to another pulse growth process, such as laser ablation, the amount of material evaporated per pulse for the plasma process is more than 200 times greater than the material evaporated per laser pulse. Typically, the energy per pulse in laser ablation is about 300 mJ, whereas the energy per pulse in the plasma is about 20 J. This analysis shows that the amount of material evaporated per Joule in the plasma process is more than three times greater than that for the laser ablation. In addition, the film profiles are much more uniform compared to greater than $\cos^{10}\theta$ profiles observed for laser ablated films.

ACKNOWLEDGMENT

This work was supported by the National Science Foundation, under Grant Nos. DMI-0078917 and DMI-0217939.

[1]S. Aisenberg and R. Chabot, J. Appl. Phys. **42**, 2953 (1971).
[2]R. B. Fair, J. Appl. Phys. **42**, 3176 (1971).

[3]D. M. Mattox, "Ion plating technology," in *Deposition Technology for Films and Coatings*, edited by R. F. Bunshah (Noyes, New York, 1982).
[4]J. J. Cuomo, J. M. E. Harper, C. R. Guarnieri, D. S. Lee, L. J. Attanasio, J. Angilello, C. R. Wu, and R. H. Hammond, J. Vac. Sci. Technol. **20**, 349 (1982).
[5]E. O. Hall, Proc. Phys. Soc. London, Sect. B **64**, 747 (1951).
[6]H. Oechsner, Appl. Phys. **8**, 185 (1975).
[7]P. D. Townsend, J. C. Kelly, and N. E. W. Hartley, *Ion Implantation, Sputtering and Their Applications* (Academic, New York, 1976).
[8]A. I. Vasin, A. M. Dorodnov, and V. A. Petrosove, Sov. Phys. Tech. Phys. **5**, 634 (1979).
[9]I. G. Brown and E. M. Oks, IEEE Trans. Plasma Sci. **25**, 1222 (1997).
[10]S. Witanachchi, K. Ahmed, P. Sakthivel, and P. Mukherjee, Appl. Phys. Lett. **66**, 1469 (1995).
[11]S. Witanachchi and P. Mukherjee, J. Vac. Sci. Technol. A **13**, 1171 (1995).
[12]P. Mukherjee, J. B. Cuff, and S. Witanachchi, Appl. Surf. Sci. **127–129**, 620 (1998).
[13]S. Witanachchi, Y. Ying, A. M. Miyawa, and P. Mukherjee, Mater. Res. Soc. Symp. Proc. **483**, 185 (1998).
[14]H. Schwartz and A. Tourtellotte, J. Vac. Sci. Technol. **6**, 374 (1969).
[15]K. Yukimura, R. Isono, T. Monguchi, and K. Yoshioka, J. Vac. Sci. Technol. B **17**, 871 (1999).
[16]D. Lubben, S. A. Barnett, K. Suzuki, S. Gorbatin, and J. E. Green, J. Vac. Sci. Technol. **6**, 373 (1969).
[17]S. Anders, A. Anders, and I. Brown, J. Appl. Phys. **74**, 4239 (1993).
[18]H. Ehrich, B. Hasse, M. Mausbach, and K. G. Muller, IEEE Trans. Plasma Sci. **18**, 895 (1990).